PHYSICAL REVIEW B VOLUME 39, NUMBER 14 15 MAY 1989-I

Structural properties of epitaxial $NiSi_2$ on Si(111) investigated with x-ray standing waves

J. Zegenhagen,* K.-G. Huang, and W. M. Gibson
State University of New York, Albany, New York 12222

B. D. Hunt†
GE Research & Development Center, Schenectady, New York 12301

L. J. Schowalter
Department of Physics, Rensselaer Polytechnic Institute, Troy, New York 12180

(Received 17 October 1988)

We have investigated the structure of epitaxial layers of *A*-type and *B*-type $NiSi_2$ on Si(111) with x-ray standing waves. Several samples of each type were used for the measurements with thicknesses of the silicides ranging from 6.3 to 97.6 nm which corresponds to 20 to 314 layers of $NiSi_2$. Our results agree with a model, where the $NiSi_2$ bonds, via the Si atoms, to the Si(111) surface dangling bonds, which leads to a sevenfold coordination of the Ni atoms in the first silicide layer. The distance of the first layer of nickel atoms from the Si(111) surface diffraction plane was determined with high accuracy for all samples. This distance is significantly shorter than the value of 0.352 nm calculated from bulk bond lengths for *A*-type epitaxy and *B*-type epitaxy for which values of 0.337 and 0.346 nm, respectively, were determined. This substantial difference and the amount of relaxation at the interface may promote understanding of the Schottky-barrier heights observed at both types of interfaces.

INTRODUCTION

There is significant interest in metal-semiconductor interfaces, which is stimulated by their importance in device fabrication. Epitaxial metal silicides on silicon have been intensively studied and $NiSi_2$ on Si(111) is one of the most prominent cases. The bulk lattice constant of the cubic CaF_2-type $NiSi_2$ is only 0.44% smaller at room temperature than the silicon lattice constant with $a=5.431$ Å and nickel disilicide grows on Si(111) with excellent crystalline quality but with two different orientations. For the one orientation, called *A* type, all crystal axes of the epitaxial film are aligned with the Si substrate. For the other orientation, called *B* type, the epitaxial silicide is rotated around the ⟨111⟩ crystal axis by 180° with respect to the Si substrate. A recipe has been developed to grow either the untwinned *A*-type epitaxy or twinned *B*-type epitaxy exclusively.[1] Grown as *A* type or *B* type, it is widely accepted that the silicide bonds via the silicon atoms to the Si substrate, which leaves the Ni atoms at the interface sevenfold coordinated.[2,3] Schematic drawings of the corresponding *A*-type and *B*-type Si(111)/$NiSi_2$ interfaces are shown in Figs. 1(a) and 1(b), respectively. Remarkably, the electronic properties of *A*-type and *B*-type $NiSi_2$ on Si(111) are different with the *B*-type junction typically having a higher Schottky barrier.[4–6] Of course, the silicide material grown on top of the silicon is the same for *A* type and *B* type and only the structural differences at the interface (such as second nearest neighbors, amount of relaxation, and defect structure) can be responsible for the difference in Schottky-barrier height (SBH).

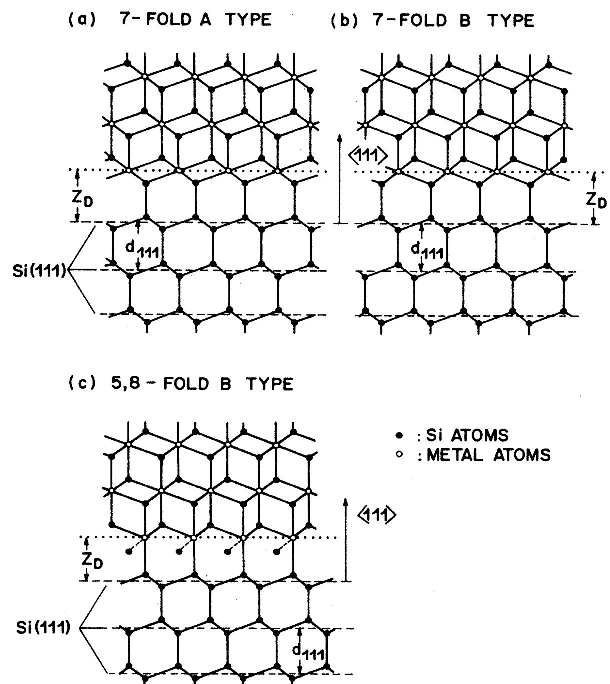

FIG. 1. Three different types of interfaces for metal silicides with CaF_2 structure on Si(111) in cross-sectional view. For details see the text.

 ©1989 The American Physical Society

The interface structure of Si(111)/$NiSi_2$ has been studied with transmission electron microscopy (TEM),[2] ion scattering,[3] the x-ray standing wave (XSW) technique,[7,8] and very recently with high-resolution x-ray diffraction.[9] Except for one XSW study,[7] there was general agreement about the sevenfold coordination of the Ni atoms at the interface. Values for the relaxation at the interface are reported for A-type[8] and B-type[3,8,9] Si(111)/$NiSi_2$ showing a decrease in the interface bond lengths. The present study is important in part because of the controversial XSW results.[7,8] In addition, by using a different experimental approach, we obtain very accurate values for the interface relaxation for A-type and B-type epitaxy. The observed magnitude and difference in relaxation may be valuable in explaining the SBH's found for the two types of epitaxy.

In a recent publication,[10] we applied bulk x-ray diffraction and the XSW technique to confirm that $CoSi_2$ bonds to the Si(111) surface via the metal atoms of the silicide [cf. Fig. 1(c)] and measured with high accuracy a strong outward relaxation (0.014±0.005 nm) of the first silicide layer.[11,12] Recent theoretical investigations support the eight-fold coordination of the Co atoms at this interface.[13,14] Our XSW results support this assignment since an extra plane of Si atoms inserted at the interface [cf. Fig. 1(c)] will tend to increase the interface distance z_D. Here we investigate the structure of Si(111)/$NiSi_2$ interfaces again with the XSW technique. The perpendicular overlayer mismatch $M_E^\perp$ of the samples has been determined independently by x-ray diffraction.[15] As we will show in some detail in the next chapter, the interface distance z_D (cf. Fig. 1) and the lattice mismatch are not parameter independent in the XSW data analysis. To fully benefit from the high structural resolution of the XSW technique, the perpendicular lattice mismatch $M_E^\perp$ of the epitaxial layer has to be determined accurately by other experimental means. This is necessary for each individual sample, because $M_E^\perp$ depends strongly on sample type (A or B), thickness of the epilayer, and details of thermal history during growth.[15]

In the present study we investigated a number of specimens with both silicide orientations (A and B) and with a large range of thicknesses of the epilayers. The interface relaxation for each individual sample was determined with high accuracy and the values obtained for samples of the same type (A or B) but with different overlayer thickness are consistently the same. The coherent fractions observed for the thicker films match the coherent fractions expected for a perfect, pseudomorphic film very well. In particular, the XSW results on the thickest (97.6 nm) $NiSi_2$ sample demonstrate the excellent crystalline quality of the epitaxial films. The misfit dislocations at the interface are practically invisible for the ⟨111⟩ XSW measurements, which confirms that their associated Burgers vectors lie in the (111) plane.[16] Furthermore, we learn from the high coherent fractions that the x-ray-interference field, which is only created if the incident and reflected x-ray waves couple coherently, extends at least 0.1 μm outside the substrate crystal surface.

In the following we will first explain how to apply the XSW analysis to epitaxial layers. Then we will briefly describe sample preparation and the experimental arrangement for XSW measurements which had been performed at the AT&T X15A beamline at the National Synchrotron Light Source (NSLS). Finally, the results of the XSW measurements are discussed in detail.

XSW ANALYSIS

The analysis of XSW data is based on the dynamical theory of x-ray diffraction, which is described in its most elegant and widely adopted form by Laue.[17] The XSW technique was developed by pioneering experiments of Batterman[18,19] and Golochenko *et al.*[20] The basic principle of the XSW technique and data analysis is described in a number of publications.[18–21] In the present study we apply the XSW technique by using the (111) reflection from the Si substrate crystals and monitoring the Ni $K\alpha$ fluorescence yield from the epilayers as a function of angle θ within the angular range of strong Bragg reflection.

The normalized, angular-dependent, fluorescence yield Y_F of a single layer of atoms located at a distance z_D from the unrelaxed substrate surface plane (cf. Fig. 1) is given as a function of angle θ by

$$Y_F(\theta)=1+R(\theta)+2\sqrt{R(\theta)}\cos[v(\theta)-2\pi z_D/d_{111}] . \tag{1}$$

In Eq. (1), $R(\theta)$ is the substrate reflectivity, $d_{111}=0.3136$ nm is the Si(111) diffraction-plane spacing, and $v(\theta)$ is the phase difference between the incident and reflected electromagnetic x-ray waves. This phase changes by π radians while passing through the angular range of Bragg total reflection. In the case of an epitaxial silicide film, a larger number of metal planes are on top of the substrate surface. The position z_n of the nth plane of metal atoms relative to the Si(111) bulklike surface plane is determined by

$$z_n=z_D+(n-1)d_E . \tag{2}$$

The lattice spacing of the epitaxial film d_E is related to the substrate lattice spacing d_{111} via

$$d_E=d_{111}(1+M_E^\perp) , \tag{3}$$

where $M_E^\perp$ denotes the perpendicular, i.e., ⊥(111), lattice mismatch of the epilayer with respect to the substrate.

The angular-dependent fluorescence yield Y_F from all the N_L layers of metal atoms of the epitaxial $NiSi_2$ film can be expressed as

$$Y_F=1+R(\theta)+2\sqrt{R(\theta)}D_w(S_c+S_u) , \tag{4}$$

where the Debye-Waller factor D_w now also takes into account thermal vibrations of the Ni atoms. This yield is again normalized with $Y_F=1$ for $R(\theta)=0$. The two sums S_c and S_u are explained in the following.

The first sum

$$S_c=\frac{1-U}{N_L}\sum_{n=1}^{N_L}\cos\{v(\theta)-2\pi[z_D+(n-1)d_E]/d_{111}\} \tag{5}$$

represents the correlated fraction of the Ni atoms, i.e., the Ni atoms which are registered perfectly in the N_L metal planes of the silicide. It is a summation representing the fluorescence contributions of the perfectly registered Ni atoms from all N_L planes. The sum

$$S_u = U/N_u \sum_{j=1}^{N_u} \cos[v(\theta) - 2\pi z_j] \tag{6}$$

is needed in a realistic model and takes into account some disorder in the epitaxials films which, though exhibiting high crystalline quality, are not perfect. This sum represents a fraction U, with $0 < U < 1$, of the metal atoms randomly distributed with respect to the lattice planes. The coordinate z_j of those atoms normal to the (111) surface is a random, real number with $0 < z_j < T_L$, where T_L is the thickness of the epilayer. The total number of randomly distributed Ni atoms is given by N_u and the random fraction U is simply given by

$$U = N_u / N_T \ , \tag{7}$$

where N_T is the total number of metal atoms sampled by XSW. Since N_T is very large (usually $N_T > 10^{13}$) it is now easy to see from Eq. (6) that, to a high degree of accuracy, $S_u = 0$ independent of the size of N_u because either $U \approx 0$ or the sum of the random-phase cosine terms equals zero. Thus we can write Eq. (4) as

$$Y_F = 1 + R(\theta) + 2\sqrt{R(\theta)}(1-U)D_w/N_L \times \sum_{n=1}^{N_L} \cos\{v(\theta) - 2\pi[z_D + (n-1)d_E]/d_{111}\} \ . \tag{8}$$

From basic trigonometry we know that a sum of cosine terms which differ only by phase factors yields again a cosine function, the amplitude and phase of which are determined by the individual phase factors in the sum. Thus we can express Y_F as

$$Y_F = 1 + R(\theta) + 2\sqrt{R(\theta)} f_c \cos[v(\theta) - 2\pi\Phi_c] \ , \tag{9}$$

where the factor $(1-U)D_w/N_L$ is contained in the amplitude f_c as well. In fact, it can be shown[21] that every result of a XSW measurement performed on a reasonably thin epitaxial layer or adsorbate can, in terms of the angular-dependent fluorescence yield Y_F, be described in the way given by Eq. (9). The amplitude factor f_c is called the coherent fraction and the phase factor Φ_c is called the coherent position. The relationship of these two quantities with the structural parameters of the epitaxial film is given in the following.

Comparing Eq. (8) and Eq. (9), with some fundamental algebra and the help of Eq. (3), we obtain

$$\Phi_c = z_D/d_{111} + (N_L - 1)M_E^{\perp}/2 + \phi_0 \ , \tag{10a}$$

$$z_D = \Phi_c d_{111} - (N_L - 1)M_E^{\perp} d_{111}/2 - \phi_0 d_{111} \ , \tag{10b}$$

and

$$f_c = (1-U)D_w |A_G| \ , \tag{11}$$

where

$$A_G = [\sin(\pi N_L M_E^{\perp})]/[N_L \sin(\pi M_E^{\perp})] \ , \tag{12}$$

$$\phi_0 = -[\mathrm{sgn}(A_G) - 1]/4 \ , \tag{13}$$

and finally,

$$N_L = T_L/[d_{111}(1 + M_E^{\perp})] \ . \tag{14}$$

The fluorescence counts $(Y_F)_{\mathrm{expt}}$, which are experimentally determined as a function of angle by the XSW measurement, are simply proportional to the yield defined by Eq. (9); thus

$$(Y_F)_{\mathrm{expt}} = C_{\mathrm{Ni}} Y_F \ . \tag{15}$$

The normalization factor C_{Ni} is proportional to the number of nickel atoms within the range of the interference field and thus to the number N_L of metal layers of the silicide film.

For the analysis of XSW data, a function as given by Eqs. (15) and (9) is fitted to the experimental data. The reflectivity $R(\theta)$ and the phase $v(\theta)$ are calculated using the formalism of the dynamical theory of x-ray diffraction.[17] It is important to note that only the three parameters C_{Ni}, f_c, and Φ_c are necessary to fit the fluorescence data if the angular scale has been determined. In the present case, this is most accurately done by fitting a theoretical expression for $R(\theta)$ to the experimentally determined reflectivity $R_{\mathrm{expt}}(\theta)$.

From Φ_c and Eq. (10b) we can now calculate z_D if the silicide thickness T_L and epilayer mismatch $M_E^{\perp}$ had been determined previously with the necessary accuracy by other experimental techniques. Using Eq. (11), we also obtain information about the crystalline quality of the films and the Debye-Waller factor of the metal atoms since A_G [compare Eq. (12)] is determined solely by the overlayer mismatch and the thickness of the film.

EXPERIMENT

Epitaxial layers of $NiSi_2$ were grown on 7.5-cm-diam, 250-μm-thick Si(111) wafers in a commercial molecular-

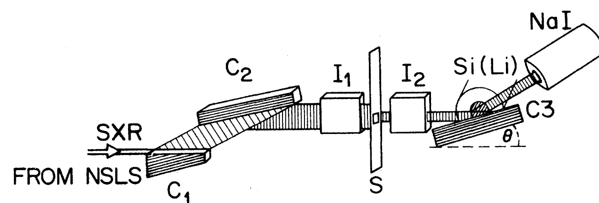

FIG. 2. Schematical experimental arrangement for XSW measurements at a synchrotron source. The white synchrotron x-ray (SXR) beam is premonochromatized and collimated in angle by an asymmetrically cut Si crystal (C_1). Grazing incidence also reduces the heat load. By fine tuning the Bragg angle of the second crystal (C_2), only one line of the harmonic spectrum of the first crystal is transmitted. The beam then passes horizontally though ion chambers (I_1 and I_2), the slit system (S), and on to the sample ($C3$).

TABLE I. Experimental results obtained on all investigated $NiSi_2$ overlayers on Si(111).

Type	Thickness (nm)	$10^2 M_E^{\perp}$	N_L	Φ_c	f_c	z_D (nm)
B	6.3	−0.75[a]	20.3	0.03	0.71	0.346
	±0.3	±0.15	±1.0	±0.01	±0.05	±0.005
B	22.5	−0.75	72.3	0.84	0.42	0.347
	±1.1	±0.01	±3.6	±0.01	±0.05	±0.004
B	97.6	−0.82	314	0.82	0.17	0.345
	±4.9	±0.01	±16	±0.02	±0.04	±0.02
A	23.3	−0.70	74.8	0.83	0.53	0.341
	±1.2	±0.01	±3.7	±0.01	±0.05	±0.005
A	22.6	−0.65	72.1	0.84	0.54	0.336
	±1.1	±0.01	±3.6	±0.01	±0.05	±0.005
A	53.2	−0.75	171	0.91	0.20	0.330
	±2.7	±0.01	±9	±0.02	±0.04	±0.010

[a]The overlayer mismatch $M_E^{\perp}$ was not determined experimentally, and we assumed the noted value with sufficient margins of error.

beam epitaxy system. Templates were formed by room-temperature deposition of 1.6–1.8 nm of Ni for *A*-type samples and 2 nm of Ni followed by 3–4 nm of Si for *B*-type samples. The wafers were subsequently annealed at 500±25 °C for 5 min. Silicide layers with the desired thickness were grown on the as-prepared templates. Deposition of Ni, or codeposition of Ni and Si for the thicker layers, was carried out with the samples held at 625±25 °C. Specimens were obtained from the large wafers by cleaving. This procedure did not strain the samples as shown by undistorted rocking curves recorded from samples cleaved from a clean wafer without an epilayer. During the growth, the thickness of the layers could be determined with an accuracy of about 10%. Thickness calibration with 5% accuracy was obtained by quantitative, x-ray-induced fluorescence analysis which was calibrated by Rutherford backscattering.

The experimental setup for the x-ray measurements at the synchrotron source, which is shown schematically in Fig. 2, will only be described briefly since it is described in more detail elsewhere.[10,22] The white beam from the NSLS x-ray ring was monochromatized and collimated in angle by Bragg reflecting from two Si(111) crystals C_1 and C_2. The current output from ionization chamber I_1 was used as a feedback signal to keep the monochromator crystals C_1 and C_2 parallel. This was achieved with a piezoelectric transducer rotating the second crystal within a narrow angular range under the control of an analog feedback circuit.[23] The second ionization chamber allowed the measurement of the beam intensity incident on the sample. The slit system was used to restrict the beam to a desired area on the sample surface. The cross section of the beam was only 10^{-2} mm^2 or smaller in order to obtain nearly undistorted rocking curves from the samples. The crystal structure of the Si substrates was still free of defects after the preparation but, because of the strain in the overlayer, the thin, triangular shaped specimens were bent spherically. For some samples, the bending radii were deduced from rocking curve measurements and found to be of the order of 10 m.

A NaI(Tl) detector monitored the reflected beam

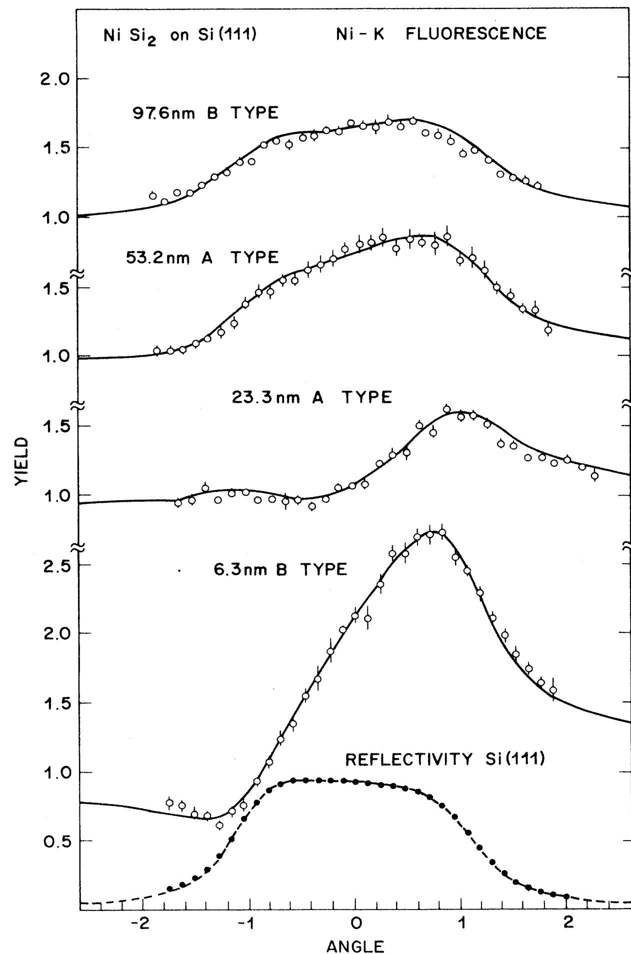

FIG. 3. XSW results on four samples. Since the scans were performed at different energies around 10 keV, the scans are shown on the energy-independent angular η scale (Ref. 18). Note that the fluorescence curves are shifted vertically on the yield axis. Symbols are the experimental data and the lines are the fitted curves.

whereas photons scattered inelastically and diffuse from the sample were detected by a Si(Li) solid-state detector. For each XSW measurement the intensity of the reflected beam as well as energy dispersive spectra from the Si(Li) containing the K fluorescence lines from the Ni were recorded simultaneously for 32 angular intervals as a function of reflection angle θ.

The results of XSW measurements for four different samples are shown in Fig. 3. A total of six samples was investigated and the results of the data analysis are compiled in Table I. Values for the perpendicular lattice mismatch $M_E^{\perp}$ of the investigated epilayers, although already published,[15] are listed as a matter of convenience in Table I too.

DISCUSSION OF RESULTS

Let us first concentrate on the information we can deduce from the observed values for f_c. With Eq. (12), we calculate A_G as a function of N_L which is obtained with Eq. (14) from T_L and $M_E^{\perp}$ for layers with the four different values of $M_E^{\perp}$. The results are shown in Fig. 4 and the values for f_c as obtained from the XSW measurement for the six individual samples are also shown in the graphs. The overall agreement between A_G and f_c is good, which proves that the $NiSi_2$ films grow layer by layer in an orderly fashion. The Debye-Waller factor must be close to unity because $f_c \approx A_G$ for the two thickest layers [compare Eq. (11)].

On a first view, the high coherent fractions observed for the thicker films represent a surprise. It is well known[24,25,15] that misfit dislocations are formed at the $NiSi_2$/Si interface in order to decrease the strain energy in the overlayer which is a result of the lattice mismatch. The dislocation density (DD) is larger for B-type layers than for A-type layers, which can even grow dislocation free up to a certain thickness.[25] Since the strain energy increases with thickness, the DD increases with thickness too. Obviously, the increasing DD does not cause a decrease in the coherent fraction. This seems to be strong evidence that the Burgers vectors characterizing the dislocations at the A- and B-type interface are both planar with respect to the (111) surface, and the defects are invisible when using a $\langle 111 \rangle$ diffraction vector.

The agreement between f_c and A_G is, in general, better for the thicker samples, which shows that the randomly distributed fraction U of the Co atoms is larger for the thinner epilayers. Possible sources for U are bulk dislocations, point defects, and of particular importance for the thinner samples, surface disorder, due to, for example, oxygen attack.

Next we calculate z_D (Ref. 26) from the experimental results using Eq. (10b) and list the values also in Table I. From the models shown in Fig. 1, it is easy to calculate values for z_D which are expected from the different geometries. Ignoring the small difference in bond length between Si—Si and Ni—Si, we obtain for geometry (a) the same distance as for (b) with

$$z_{D7} = 9/8 d_{111} = 0.352 \text{ nm} \quad (16)$$

and for geometry (c)

$$z_{D5} = 7/8 d_{111} = 0.274 \text{ nm} . \quad (17)$$

Obviously z_{D7} agrees well with the experimental results, and we conclude, given the choice between model (a) or (b) and (c) of Fig. 1, that the Ni atoms are sevenfold coordinated at the interface. The values for z_D agree well for layers of the same orientation but are clearly different between the A- and B-type epitaxy. The two average values $\langle z_D \rangle$ from the three measurements for each type of layers are listed in Table II. Also listed are the differences $\Delta z_D = \langle z_D \rangle - z_{D7}$ which we take as a measure for the relaxation at the interface. For both types of silicides, Δz_D is significantly smaller than zero but the compression at the interface is much more pronounced for the A type.

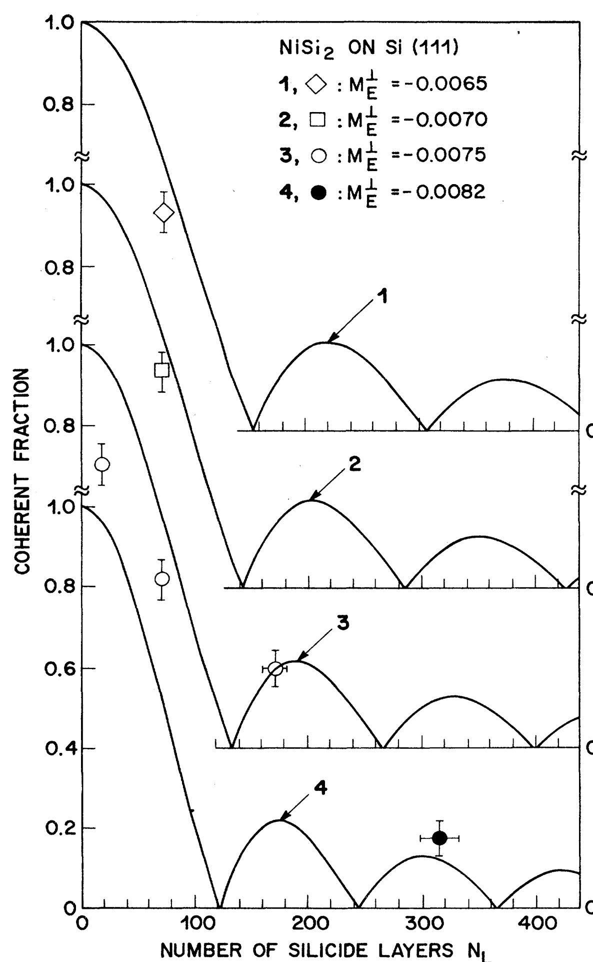

FIG. 4. Coherent fraction as a function of $NiSi_2$ layer thickness with the four different mismatch values from Table I as parameter. The solid lines are calculated curves according to Eqs. (11) and (12) with $U=0$ and $D_w = 1.0$. Curves 1, 2, and 3 are shifted on the vertical axis. Symbols are experimentally determined coherent fractions. The theoretical curves clearly show the interference beating between the standing x-ray-wave field with periodicity d_{111} and the epitaxial layers with periodicity $d_E = (1 + M_E^{\perp}) d_{111}$.

TABLE II. Surface bond length z_D (cf. Fig. 1) and interface relaxation Δz_D for A- and B-type $NiSi_2$ on Si(111). Results for the interface relaxation obtained by other groups are also listed.

	z_D, experiment (nm)	Present study Δz_D (nm)	Ref. 3 Δz_D (nm)	Ref. 8 Δz_D (nm)	Ref. 9 Δz_D (nm)
A type	0.337	−0.016	NA[a]	−0.004	NA
	±0.005	±0.005		±0.005	
B type	0.346	−0.007	−0.006	−0.011	−0.008
	±0.003	±0.003	±0.008	±0.003	±0.006

[a]NA is not available.

The 0.009-nm difference in the interface relaxation observed for the two types of $NiSi_2$ may be related to about 0.14 V difference in SBH found for A- and B-type interfaces.[4–6] For the magnitude of the relaxation at the interface, Vlieg *et al.*[8] reported larger values for B type than for the A type, in disagreement with our findings. However, they investigated only a total of three samples and determined z_D and $M_E^{\perp}$ solely from the XSW results using the dependency of Φ_c on N_L as given by Eq. (21a). In this way, they implicitly assumed $M_E^{\perp}=\text{const}$ for all specimens and neglected that $M_E^{\perp}$ depends on layer type and thickness and even on sample preparation since slightly different growth conditions can readily cause differences in the densities of defects which in turn affects $M_E^{\perp}$.[15]

CONCLUSION

The present XSW measurements have been performed on epitaxial layers of $NiSi_2$ on Si(111) more than 300 layers thick. The good agreement between calculated and measured coherent fractions demonstrates the excellent epitaxial quality of the films. From the results of the analysis of the XSW data we can clearly rule out that the investigated epilayers bond to the Si(111) surface dangling bonds via the metal atoms. Our results agree well with the widely accepted interface structure where the silicide bonds to the Si(111) surface dangling bonds via the Si atoms, which results in sevenfold coordinated Ni atoms at the interface. If we assume bulklike bond length and calculate the distance of the first Ni layer from the Si(111) surface which is assumed to be in a bulklike position and compare it with the experimental determined distances, we find that the experimental determined values are significantly smaller. In case of the A-type epitaxy, the $NiSi_2$ film is relaxed by 0.016±0.005 nm towards the Si crystal while the inward relaxation at the B-type interface with 0.007±0.005 nm is less strongly pronounced. The 0.009-nm difference in interface relaxation is expected to bear on issues such as the theoretical understanding of the difference in SBH observed for A- and B-type epitaxy.

ACKNOWLEDGMENTS

We gratefully acknowledge valuable assistance by B. M. Kincaid and J. B. Mock at the X15A beamline. This work was supported by the National Science Foundation under Grant No. DMR 8017303.

*Present address: AT&T Bell Laboratories, Murray Hill, NJ 07974.

†Present address: JPL, Caltech, Pasadena, CA 91109.

[1]R. T. Tung, J. M. Gibson, and J. M. Poate, Phys. Rev. Lett. **50**, 429 (1983).

[2]D. Chems, G. R. Anstis, J. L. Hutchinson, and J. C. H. Spence, Philos. Mag. A **46**, 849 (1982).

[3]E. J. van Loenen, J. W. M. Frenken, J. F. van der Veen, and S. Valeri, Phys. Rev. Lett. **54**, 827 (1985).

[4]R. T. Tung, Phys. Rev. Lett. **52**, 461 (1984).

[5]R. J. Hauenstein, T. E. Schlesinger, T. C. McGill, B. D. Hunt, and L. J. Schowalter, J. Vac. Sci. Technol. A **4**, 860 (1986).

[6]M. Ospelt, J. Henz, L. Flepp, and H. von Känel, Appl. Phys. Lett. **52**, 227 (1988).

[7]K. Akimoto, T. Ishikawa, T. Takahashi, and S. Kikuta, Jpn. J. Appl. Phys. **24**, 1425 (1985).

[8]E. Vlieg, A. E. M. J. Fischer, J. F. van der Veen, B. N. Dev, and G. Materlik, Surf. Sci. **178**, 36 (1986).

[9]I. K. Robinson, R. T. Tung, and R. Feidenhans'l, Phys. Rev. B **38**, 3632 (1988).

[10]J. Zegenhagen, K.-G. Huang, B. D. Hunt, and L. J. Schowalter, Appl. Phys. Lett. **51**, 1176 (1987).

[11]Fischer *et al.* (Ref. 12) reported a much smaller relaxation (0.005±0.003 nm) for the first Co layer at the Si(111)/$CoSi_2$ interface. The study was performed in the same way as the work on $NiSi_2$ by Vlieg *et al.* (Ref. 8), which is discussed later.

[12]A. E. M. J. Fischer, E. Vlieg, J. F. van der Veen, M. Clausnitzer, and G. Materlik, Phys. Rev. B **36**, 4769 (1987).

[13]D. R. Hamann, Phys. Rev. Lett. **60**, 313 (1988).

[14]P. J. van den Hoek, W. Ravekek, and E. J. Baerendo, Phys. Rev. Lett. **60**, 1743 (1988).

[15]J. Zegenhagen, M. A. Kayed, K.-G. Huang, W. M. Gibson, J. C. Philips, L. J. Schowalter, and B. D. Hunt, Appl. Phys. A **44**, 365 (1987).

[16]F. Föll, P. S. Ho, and K. N. Tu, J. Appl. Phys. **52**, 250 (1981).

[17]M. v. Laue, *Röntgenstrahlinterferenzen,* 3rd ed. (Akademische Verlagsgesellschaft, Frankfurt, 1960).

[18]B. W. Batterman, Phys. Rev. **133**, A759 (1964).

[19]B. W. Batterman, Phys. Rev. Lett. **22**, 703 (1969).

[20]J. A. Golovchenko, B. W. Batterman, and W. L. Brown, Phys. Rev. B **10**, 4239 (1974).

[21]N. Hertel, G. Materlik, and J. Zegenhagen, Z. Phys. B **58**, 199 (1985).

[22]J. Zegenhagen, J. R. Patel, B. M. Kincaid, J. A. Golovchenko, J. B. Mock, P. E. Freeland, and R. J. Malik, Appl. Phys. Lett. **53**, 252 (1988).

[23]A. Krolzig, G. Materlik, M. Swars, and J. Zegenhagen, Nucl. Instrum. Methods **219**, 430 (1984).

[24]R. A. Hamm, J. M. Vandenberg, J. M. Gibson, and R. T. Tung, Mater. Res. Soc. Symp. Proc. **37**, 367 (1985).

[25]M. Okamoto, S. Hashimoto, B. D. Hunt, L. J. Schowalter, and W. M. Gibson, Mater. Res. Soc. Symp. Proc. **56**, 157 (1986).

[26]Note that the quantity z_D determined by the data analysis gives exactly the distance of the first Ni layer from the Si(111) surface if no relaxation occurs at either the Si(111) or the $NiSi_2(111)$ interface surfaces.